

A NOVEL MULTI-STATE INTEGRATED RF MEMS SWITCH FOR RECONFIGURABLE ANTENNAS APPLICATIONS

Ali Pourziad^{*}, Saeid Nikmehr, and Hadi Veladi

Faculty of Electrical and Computer Engineering, University of Tabriz, Tabriz, Iran

Abstract—A novel multi-state RF MEMS switch for microstrip antenna applications is presented. The proposed switch exhibits seven different states of operation, has a very simple DC biasing mechanism, and can be integrated with antenna structure. Based on these properties, this switch may find its usage in multifunction reconfigurable antennas. To exhibit this application, it is employed in the reconfiguration mechanism of a U-slotted antenna. In different states of the switch, the antenna resonates at different frequencies. All the standard frequency bands of the wireless communication services with some additional frequency bands is covered with this reconfigurable U-slotted antenna. Moreover, the proposed antenna structure is a cost-effective solution since it comprises a commonly used FR4 substrate. The switch is integrated with antenna structure on the same substrate. A prototype of the designed antenna was fabricated and tested for performance verification of the proposed switch and antenna.

1. INTRODUCTION

Development of high performance modern wireless communication systems has resulted in the tremendous increase in the number of antennas which are used as a critical part of these systems. They are necessary for supporting different radiation characteristics of the multi-standard wireless communication services. Cost effectiveness, low power consumption, compact size and tunability are desirable features in these systems [1, 2]. The tunability sometimes makes the system act as an intelligent system. Software defined radios

Received 23 January 2013, Accepted 28 March 2013, Scheduled 1 May 2013

* Corresponding author: Ali Pourziad (ali.pourziad@tabrizu.ac.ir).

(SDRs), adaptive multiple-input multiple-output (MIMO) wireless communication systems and Cognitive Radios are examples of smart systems in which the tunability is indispensable [2–4]. The tunability property is also known as reconfigurability characteristic. Reconfigurable devices such as antennas [1–14], filters [15–19], impedance tuners [20–23], phase shifters [24, 25] and amplifiers [26–29] have been used in recent years, considerably. The pattern, polarization, bandwidth and resonant frequency are fixed radiation parameters of the conventionally used antennas. In contrast, by introducing reconfigurable antennas, these parameters can be changed dynamically [2]. This reconfigurability presents some new challenges and opportunities in the antenna design. These reconfiguration mechanisms can often be achieved by employing microwave switches, such as PIN diodes [1, 10, 30–32], varactor diodes [1, 13, 33], GaAs FETs [10, 34, 35] (semiconductor active switches) and Radio Frequency MicroElectroMechanical Systems (RF MEMS) [2, 6–12]. High linearity, low power consumption, low insertion loss and good isolation are major advantages of the RF MEMS switches with respect to the semiconductor active switches [36–37].

Slot antennas are good candidates to be used as a building block in designing of reconfigurable antennas. In these antennas, by proper placement of switches on the slot, it is possible to change the radiation characteristics of antenna [1, 38–41]. This is done by changing the electrical length of the current path or manipulation of the current distribution around the slot. However, DC biasing circuits for RF MEMS switches introduce some interference with the RF radiating mechanism. For slot antennas, the DC biasing circuits are the drawback in design of the reconfigurable antennas. To overcome this problem, floating DC ground and integrated DC biasing have been introduced. In the former case, due to floating ground, the fully integrated antenna is not achievable [40]. In the latter case, either commercially packaged switches are used or the RF MEMS switches are themselves integrated in the structure of the antenna. For both packaged and integrated switch types, the DC biasing circuits are integrated in the antenna structure. By incorporating these circuits in antenna structure, the overall dimension of the antenna is increased, significantly. In addition, these designs also need some DC blocking circuits and filters that in turn result in a complicated structure.

Necessity of wire bounding, impedance mismatch and signal loss at the interface between the packaged switch and the antenna board are some problems of the Packaged switches [42]. Initially, the integrated switches were implemented on commonly used Si or glass substrates for electronic boards [24]. Some antennas have

been designed monolithically on these substrates by RF MEMS switches [43]. However, these boards have high permittivity and their radiation characteristics are not desirable. Monolithic integration of the RF MEMS switches with antenna structure on the antenna's low permittivity substrates, especially on the PCB boards, makes them very attractive and popular in design of reconfigurable antennas [44].

Two different types of RF MEMS switches are commonly used in design of the reconfigurable antennas, the shunt and series types [36]. These switches have two states of 'On' and 'Off' operation, for which two degrees of freedom are achievable. This feature limits the tunability capability of the switch and results in incremental number of the switches due to more reconfigurability requirements which in turn results in complicated antenna structure. In this paper, a novel RF MEMS switch with a simple DC biasing circuits and multi-state functionality is proposed. To demonstrate its performance, a simple U slot rectangular patch antenna is selected, and the proposed novel switch is implemented in its structure on a via in the slot.

2. STRUCTURE OF THE RF MEMS SWITCH

The structure of the proposed switch as shown in Figure 1(a), comprises three beams (membranes) and a conductor via. There are two possible choices of switch excitation. When the beams are of different sizes, only one conductor pin can be used to feed all three beams and to provide a rout for their different actuation voltages. In this case, the switch would work at sequential states. However,

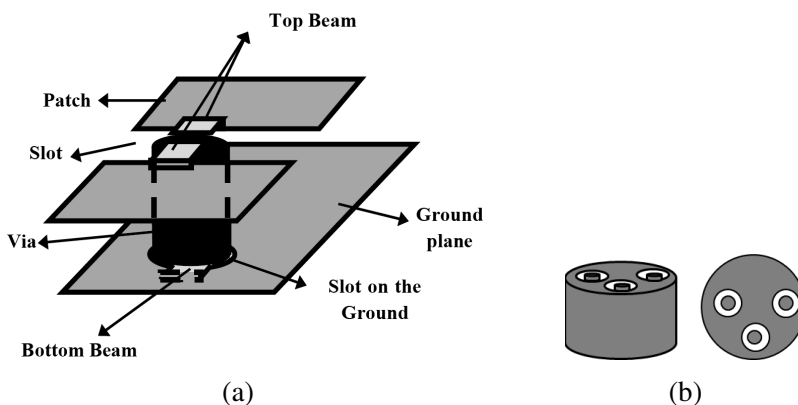






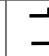
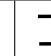
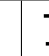
Figure 1. (a) Schematic structure of the switch, (b) side and top views of excitation pins.

for the same sized beams, separate pins which are located inside the holes in conductor via must be used to excite an individual beam (Figure 1(b)). In this case, the switch may be operated in any desired state. In either case, the upper and bottom beams are connected to the patch and ground plane, respectively. Therefore, the DC ground must be connected to both patch and ground plane. The actuating voltage is then applied to the pins from lower side of the structure, to avoid interaction with RF mechanism of the structure in antenna applications. As a result, the need for DC biasing circuits is eliminated, and the switch can be fully integrated in the structure of a reconfigurable antenna.

Here, we employ the second excitation mechanism in which the switch exhibits different states of operation depending on the positions of its three beams. Each beam has two different modes of operation when located at ‘Up’ or ‘Down’ positions. At ‘Down’ location, the beam is connected to its pin, and at ‘Up’ situation, the beam is suspended over the via. Table 1 presents the seven possible states of the switch. It should be noted that when both top beams are at the ‘Up’ position, the effect of the ‘Up’ or ‘Down’ locations of the bottom beam are the same. Therefore, here, only one of these two states is considered, which makes the number of the states seven instead of eight.

The simulation model of the proposed switch in Ansoft HFSS Software is shown in Figure 2. For all beams, the dimensions of

Table 1. Various states of the switch.

State	1	2	3	4	5	6	7
T. Beam 1	Up	Down	Down	Down	Up	Up	Down
T. Beam 2	Up	Up	Down	Down	Down	Down	Up
B. Beam	Up	Up	Up	Down	Up	Down	Down
Schematic diagram							

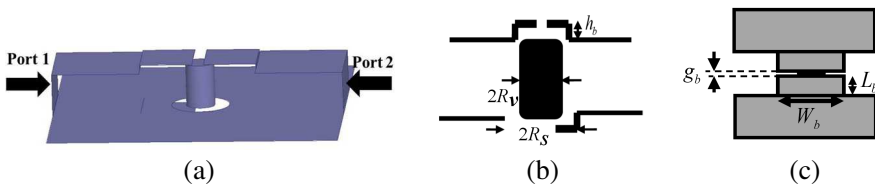


Figure 2. The simulation model of the switch: (a) 3-D view, (b) side view, (c) top view.

$R_v = 0.5$ mm, $R_s = 1$ mm, $W_b = 2$ mm, $L_b = 1.8$ mm, $g_b = 0.4$ mm and $h_b = 0.02$ mm are chosen. These dimension choices are consistent with those of commonly used available commercial RF MEMS switches. A low cost FR4 board with thickness of 1.6 mm is taken for the substrate of the switch.

The $|S_{21}|$ parameter of the switch is selected to compare its performance at four different states of Table 1. The simulation results of the states 1, 2, 4 and 6 are shown in Figure 3(a). Note that for symmetric characteristics of the switch, its operation at states 2 and 6 are similar to states 5 and 7, respectively. It is obvious that only when both top beams are at down locations and bottom beam at up position, the switch is ON (state 3). The result of the simulation for state 3 is shown in Figure 3(b). Simulation results show that as the frequency increases, the performance of the switch goes away from its ideal operation (low insertion losses and high isolation at ON and OFF states, respectively). By increasing the frequency, the electrical dimensions of the beams and conductor pins increase and these structures can radiate. Therefore, frequency increment causes the deviation of the switch's operation from its ideal task. To verify

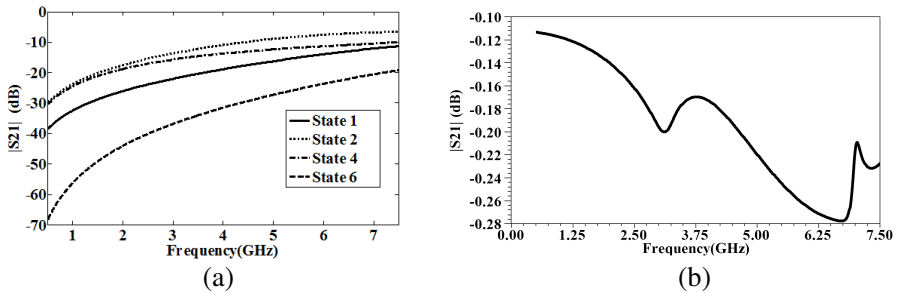


Figure 3. $|S_{21}|$ of the switch at: (a) various states, (b) state 3.

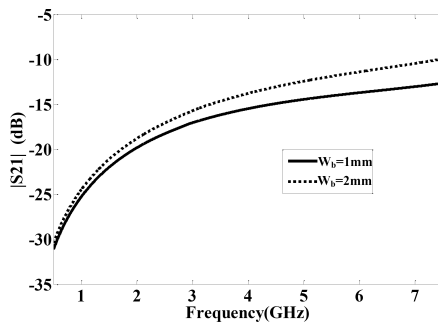


Figure 4. Effect of the beam's width of the switch.

this alteration of the operation of the switch at higher frequencies, state 4 is simulated with two different widths of the beams: 1 mm and 2 mm. From the simulation results in Figure 4, the significant deviation from ideal response at higher frequencies, due to its radiation effects, is obvious. Therefore, the choice of the sizes of beams should be based on such an study and observation of the values of insertion loss and uniformity of the response at the desired frequency band.

3. RECONFIGURABLE ANTENNA DESIGN

There are many reconfigurable antennas with complicated structures. The design methodology in most of these antennas is based on the trial

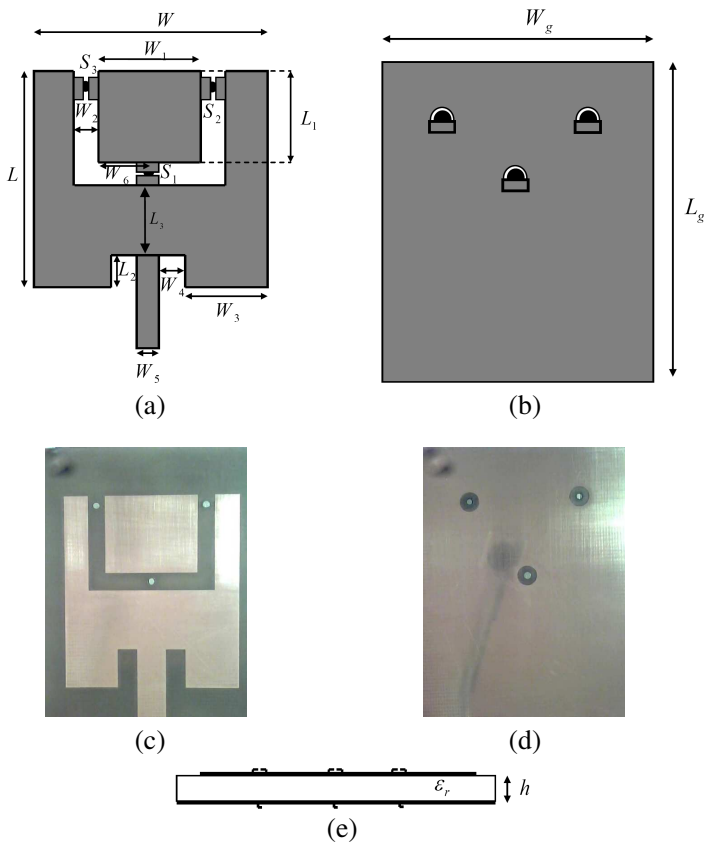


Figure 5. U-slotted antenna: (a) top view, (b) bottom view, (c) top view of the fabricated prototype, (d) bottom view of the fabricated prototype, (e) side view.

and error. However, it is more desirable that a simple basic structure, such as rectangular or circular patches, with available analytical design formulation, is selected. Then, by means of theoretical modifications a reconfigurable antenna would be achieved. Here, to present our proposed RF MEMS switch, a rectangular patch antenna is selected and a U-slotted is cut from it. The choice of the slot shape is based on the current distribution on the antenna. The schematic structure of this antenna and fabricated prototype, without RF MEMS switches, are shown in Figure 5. TM₀₁ and TM₁₀ are the fundamental modes of a rectangular microstrip antenna, where the former has longitudinal current path. In order to reduce the size of antenna, the current path of this mode should be made longer. Here a U-slotted has been cut from the rectangular patch for deforming the current path. Since the current distributions of the leading modes of this rectangular patch antenna are y and x directed, this shape of the slot can alter the current paths of both of these modes. Therefore, the resonant frequencies of these modes are changed. Here, for achieving reconfigurable characteristics, three RF MEMS switches are used on the U-slotted, as shown in Figure 5(a). The parameter values of this antenna are given in Table 2. Conductor vias have some inductance effects that are investigated in Figure 6. The results are given for the original U-slotted antenna as well as the original antenna plus conductor vias with/without ground slots beneath the vias. It is clear from this figure that the effect of the conductor vias in the presence of circular slots on the ground plane is negligible with respect to the case where the ground slots are absent.

Table 2. Parameter values of the antenna.

Parameter	L	W	L_1	L_2	L_g	W_1	W_2
Value (mm)	40	36	16	8	60	19	3.5
Parameter	W_3	W_4	W_5	W_6	W_g	h	ϵ_r
Value (mm)	11	4	6	9.5	50	3.2	4.4

Figure 6 shows that the U-slotted antenna has three operating frequency bands. The first resonance (1.8 GHz) is determined by the longitudinal length of the antenna (L). The second resonance (4.18 GHz) is determined by the antenna half width (W) while the third band (5.56 GHz and 6.37 GHz resonances) is based on the values of L_3 and W_3 . Figure 7 shows the current distributions on the antenna at these frequencies.

To achieve a frequency reconfigurable antenna, the RF MEMS switches should be placed in locations that the current paths can be affected. The antenna structure could be loaded by the middle

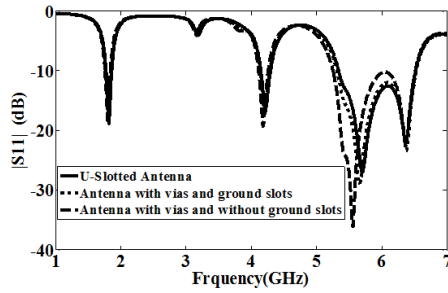


Figure 6. The effect of the conductor vias on the performance of the U-slotted antenna.

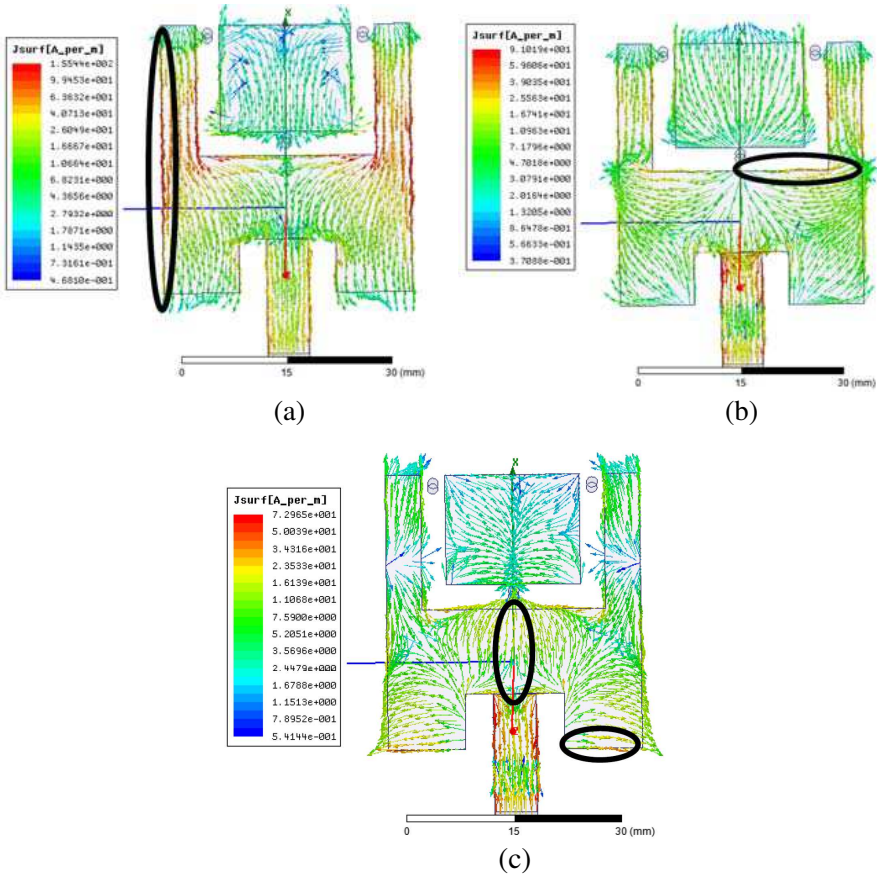


Figure 7. Current distributions on the patch: (a) 1st resonance (1.8 GHz), (b) 2nd resonance (4.18 GHz), (c) 3rd resonance (5.56 GHz).

small rectangular patch through the U-slotted. On the other hand, in the absence of switches, this small rectangular patch is a floating patch. By loading this small rectangular patch to the main part of the antenna, the electrical length of some of the current paths can become longer. This effect causes the antenna to resonate at lower frequencies. Therefore, three switches can make this antenna act as a reconfigurable structure in two manners. First, in some states of the switches, the electrical current path lengths are affected which in turn changes the resonant frequencies of the antenna. Second, in some other states of the switches the antenna is loaded by the small rectangular patch at some locations.

The locations of the switches are shown in Figure 5 where the switch S_1 is located in the middle of the horizontal section of the slot, and S_2 and S_3 are placed at the end sections of the vertical arms of the slot. Since each switch has seven states, the combination of switches would have many states. In the following, three beams of each switch are referred as inner, outer and bottom beams. The inner beam is one of the upper beams that is connected to the main part of the antenna. The other upper beam connected to the floating small rectangular patch is referred as outer beam.

Here, the states of a switch are selected based on the desired adjustment in the resonance frequencies of the antenna. For example, if it is desirable to have changes in the two upper bands without altering the first resonance, it is necessary for S_1 to change its state. Figure 8(a) shows the simulation results of $|S_{11}|$ for the antenna while S_1 is at state 2 and other switches at states 1. The schematic diagram of the switches are shown in the insert of this figure. For each switch, the left and right top beams are in fact inner and outer beams, respectively. This would be the case for the rest of the figures in this paper. It is clear that while the first resonance frequency of the antenna is unchanged, two upper ones are altered. Therefore, by changing the state of S_1 , the antenna is converted to a single band antenna. Figure 8(b) shows the simulation results of the antenna while S_1 is at state 3 and other switches are again at state 1. Similar to the previous case, the first resonance is not changed while the others are altered. In this case, the antenna is loaded by small rectangular patch that makes the antenna resonate at lower frequency. If it is desirable that the first resonance frequency is shifted, it is apparent that the states of S_2 and/or S_3 should be changed from state 1. The simulation result of the antenna, when S_2 and S_3 are at state 3 and S_1 at state 1, is presented in Figure 8(c). This situation makes the antenna loaded by the small patch. Shifting the primary resonance of the antenna and appearance of higher resonances are the results of this loading of the antenna.

Simulation results of the antenna at the states 1, 3 and 4 of S_1 , S_2 and S_3 respectively, are illustrated in Figure 8(d). Once more, as can be seen from this figure, the first resonance has been changed with respect to the previous cases, but higher bands have not been altered significantly. In these cases, the effect of the small patch at the first resonance is clear. The result for the cases that S_1 , S_2 and S_3 have, respectively, states 5, 3 and 3 has been presented in Figure 8(e). This figure approximately demonstrates the shift in all resonance frequencies as it was anticipated. The state in Figure 8(f) is similar to the previous state, but the state of S_1 is changed to 6. The radiation patterns and gain of the antenna at some states are shown in Figures 9 and 10, respectively.

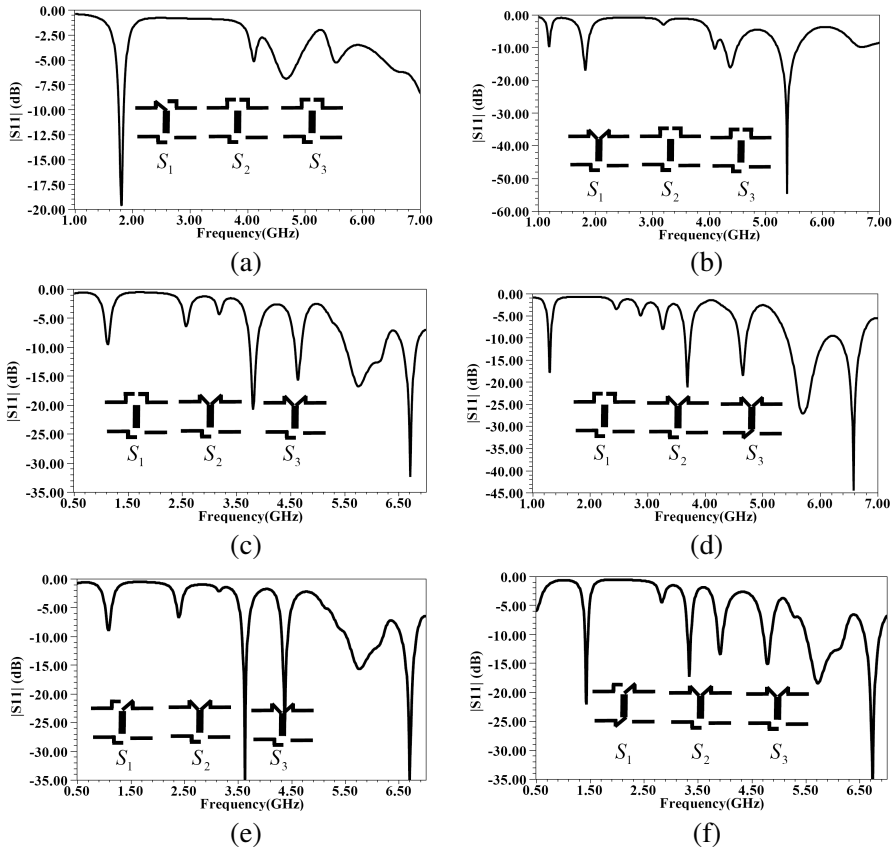


Figure 8. $|S_{11}|$ of the antenna when S_1 , S_2 and S_3 are, respectively, at states: (a) 2, 1, 1, (b) 3, 1, 1, (c) 1, 3, 3, (d) 1, 3, 4, (e) 5, 3, 3, (f) 6, 3, 3.

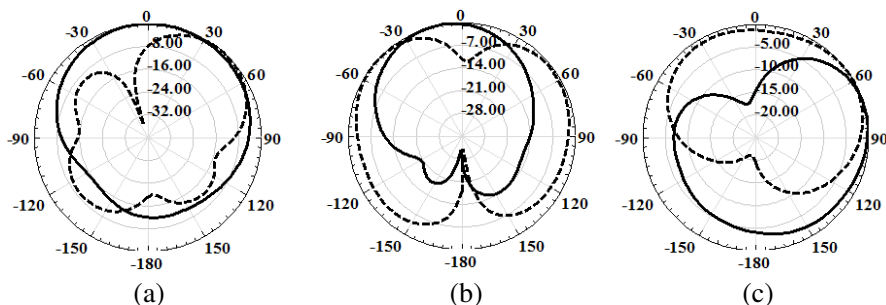


Figure 9. Normalized radiation patterns of the antenna, E -plane (solid lines), H -plane (dashed lines) at: (a) all switches are off at $f = 1.82$ GHz, (b) state of Figure 8(d) at $f = 3.7$ GHz, (c) state of Figure 8(e) at $f = 1.28$ GHz.

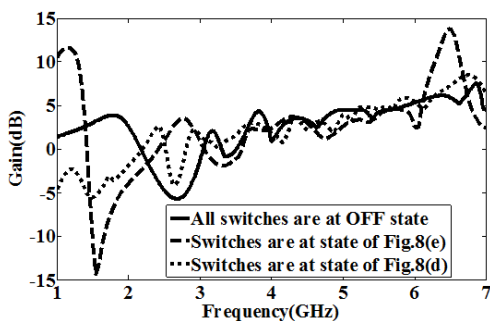


Figure 10. The peak gain of the antenna at some states.

4. EXPERIMENTAL RESULTS

A prototype of the proposed antenna with RF MEMS switches is fabricated and tested. In the simulation results of the previous section, conducting strips were used as ideal switches, and the dispersive characteristics of the substrate was ignored. Since FR4 is a dispersive substrate, and the under investigation frequency range is wide, initially by using HP8720ES vector network analyzer, the permittivity of the substrate was measured, and the results were taken into account in the simulation. The fabrication process of the designed RF MEMS switches is based on mutiple layer copper plating, while using photoresist for both the lithographic process and as a sacrificial layer for later release procedure. Starting a bare FR4 wafer, the via is drilled first using appropriate layout (Figure 11(a)). The substrate

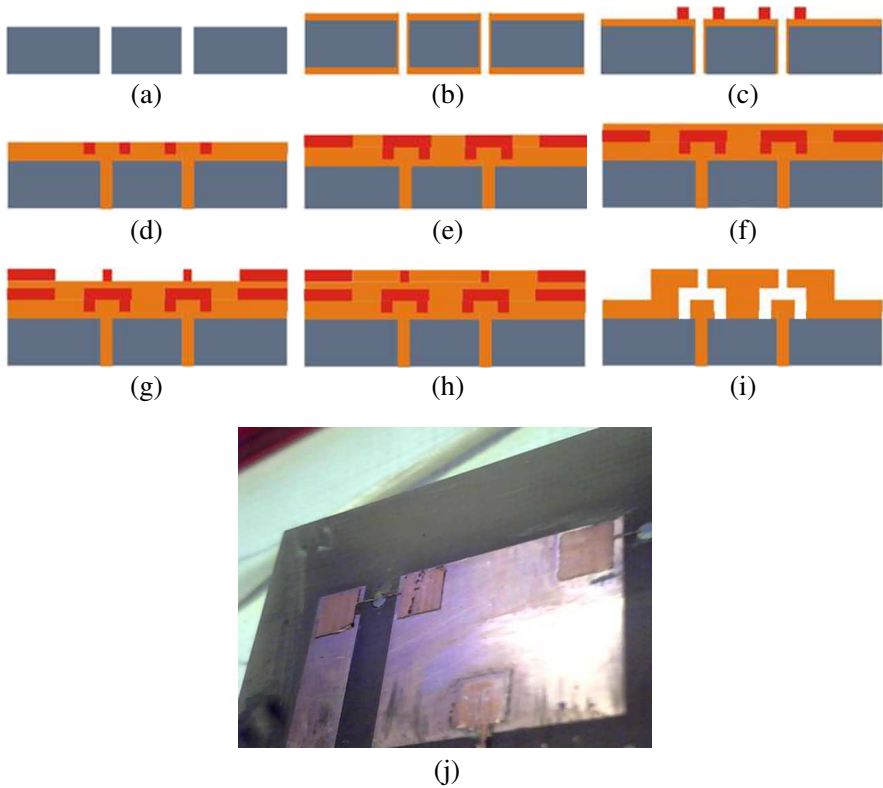


Figure 11. Fabrication procedure of the RF MEMS switches.

is then sputter coated with a thin seed layer of copper (Figure 11(b)). The patch and slot separation is then patterned on a thin photoresist layer (Figure 11(c)) which is followed by Cu electroplating to achieve a proper via and antenna component layer (Figure 11(d)). Next, the gap layer between the slot and patches are formed (Figure 11(e)) by a fresh photoresist layer, coated and patterned by the spacer layout, and then the substrate is electroplated once again by Cu up to dedicated spacer thickness. To make the cantilever beams operate as the switch arms, a subsequent Cu seed layer is required, which is formed by Cu sputtering on the substrate (Figure 11(f)). Actual beams are formed by coating the third photoresist layer, which is patterned using the beams layout (Figure 11(g)). The thickness of the third resist layer is set to the required beam parameters as discussed earlier. The final switch beams are obtained by an Cu electroplating procedure (Figure 11(h)), and eventually the whole structure is released by

stripping the photoresist (Figure 11(i)) using suitable stripper. We require a short Cu etching procedure during the release step to remove the seed Cu layer. Otherwise, it could short circuit the patch and the slot. The whole procedure can be accomplished for both sides of the substrate to form the required switches on the desired positions. Here, Dupont dry film resist, Tentmaster tm200i, is used as photoresist. The standard developing process is performed as described by the manufacturer, that is Na_2CO_3 for developing and NaOH to release the suspended cantilever beam. Figure 11(j) shows the prototype antenna with fabricated switches. Figure 12 shows the results for some states of the antenna. As can be seen, there is a good agreement between simulated and measured results.

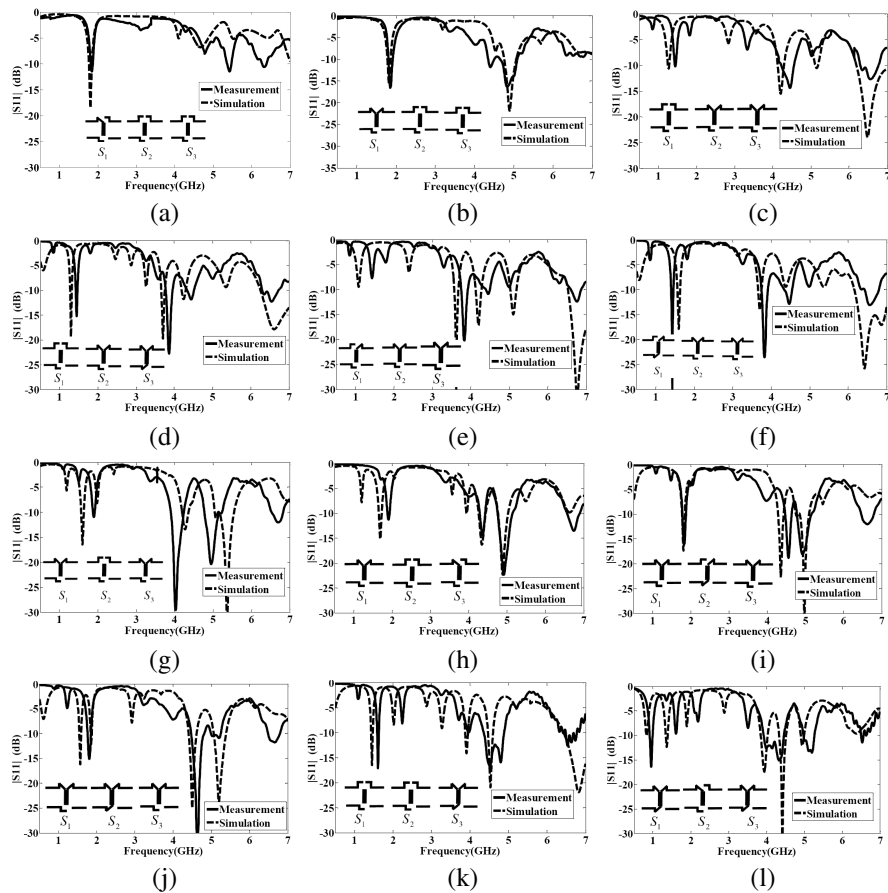


Figure 12. Measured and simulated $|S_{11}|$ at some states.

5. CONCLUSION

A novel integrated RF MEMS switch was introduced for reconfigurable antenna applications. Multi-state operation, ease of DC biasing mechanism and capability of integration with antenna structure are the major advantages of the proposed switch in comparison with the previously published reports. The operation of the proposed switch at different states was investigated. To demonstrate the application, three switches were employed on the U-slotted rectangular antenna. The locations of the switches were selected so that the resonant frequencies of the antenna can be changed based on the requirements of the user. By creating many resonance frequencies, the antenna could operate over the entire standard wireless spectra. The introduced switch can also be used in other slotted antenna configurations. A prototype of the introduced antenna was fabricated and tested. The conformity between experimental and simulated results was demonstrated.

REFERENCES

1. Tariq, A. and H. Ghafouri-Shiraz, "Frequency-reconfigurable monopole antennas," *IEEE Trans. Antennas Propag.*, Vol. 60, No. 1, 44–50, 2012.
2. Cetiner, B. A., G. R. Crusats, L. Jofre, and N. Biyikli, "RF MEMS integrated frequency reconfigurable annular slot antenna," *IEEE Trans. Antennas Propag.*, Vol. 58, No. 3, 626–632, 2010.
3. Hall, P. S., P. Gardner, J. Kelly, E. Ebrahimi, M. R. Hamid, F. Ghanem, F. J. Herraiz-Martinez, and D. Segovia-Vargas, "Reconfigurable antenna challenges for future radio systems," *Proc. 3rd Eur. Conf. Antennas Propag.*, 949–955, Berlin, Germany, 2009.
4. Oh, S. H., J. T. Aberle, S. Anantharaman, K. Arai, H. L. Chong, and S. C. Koay, "Electronically tunable antenna pair and novel RF front-end architecture for software-defined radios," *EURASIP J. Appl. Signal Process.*, Vol. 2005, 2701–2707, 2005.
5. Romano, N., G. Prisco, and F. Soldovieri, "Design of a reconfigurable antenna for ground penetrating radar applications," *Progress In Electromagnetics Research*, Vol. 94, 1–18, 2009.
6. Martinez-Lopez, R., J. Rodriguez-Cuevas, A. E. Martynyuk, and J. I. Martinez-Lopez, "An active ring slot with RF MEMS switchable radial stubs for reconfigurable frequency selective surface applications," *Progress In Electromagnetics Research*, Vol. 128, 419–440, 2012.

7. Petit, L., L. Dussopt, and J.-M. Laheurte, "MEMS-switched parasitic-antenna array for radiation pattern diversity," *IEEE Trans. Antennas Propag.*, Vol. 54, No. 9, 2624–2631, 2006.
8. Anagnostou, D. E., G. Zheng, M. T. Chryssomallis, J. C. Lyke, G. E. Ponchak, J. Papapolymerou, and C. G. Christodoulou, "Design, fabrication and measurements of an RF-MEMS-based self similar reconfigurable antenna," *IEEE Trans. Antennas Propag.*, Vol. 54, No. 2, 422–432, 2006.
9. Boyle, K. R. and P. G. Steeneken, "A five-band reconfigurable PIFA for mobile phones," *IEEE Trans. Antennas Propag.*, Vol. 55, No. 11, 3300–3309, 2007.
10. Mak, C. K., C. R. Rowell, R. D. Murch, and C.-L. Mak, "Reconfigurable multiband antenna designs for wireless communication devices," *IEEE Trans. Antennas Propag.*, Vol. 55, No. 7, 1919–1928, 2007.
11. Rajagopalan, H., R.-S. Yahya, and W. A. Imbriale, "RF MEMS actuated reconfigurable reflectarray patch-slot element," *IEEE Trans. Antennas Propag.*, Vol. 56, No. 12, 3689–3699, 2008.
12. Kingsley, N., G. E. Ponchak, and J. Papapolymerou, "Reconfigurable RF MEMS phased array antenna integrated within a liquid crystal polymer (LCP) system-on-package," *IEEE Trans. Antennas Propag.*, Vol. 56, No. 1, 108–118, 2008.
13. Shynu, S. V., G. Augustin, C. K. Aanandan, P. Mohanan, and K. Vasudevan, "Design of compact reconfigurable dual frequency microstrip antennas using varactor diodes," *Progress In Electromagnetics Research*, Vol. 60, 197–205, 2006.
14. Monti, G., L. Corchia, and L. Tarricone, "A microstrip antenna with a reconfigurable pattern for RFID applications," *Progress In Electromagnetics Research B*, Vol. 45, 101–116, 2012.
15. Vu, T. M., G. Prigent, J. Ruan, and R. Plana, "Design and fabrication of RF-MEMS switch for V-band reconfigurable application," *Progress In Electromagnetics Research B*, Vol. 39, 301–318, 2012.
16. Al-Husseini, M., L. Safatly, A. Ramadan, A. El-Hajj, K. Y. Kaban, and C. G. Christodoulou, "Reconfigurable filter antennas for pulse adaptation in UWB cognitive radio systems," *Progress In Electromagnetics Research B*, Vol. 37, 327–342, 2012.
17. Naglich, E. J., J. Lee, D. Peroulis, and W. J. Chappell, "Switchless tunable bandstop-to-all-pass reconfigurable filter," *IEEE Trans. Antennas Propag.*, Vol. 60, No. 5, 1258–1265, 2012.
18. Miller, A. and J. Hong, "Cascaded coupled line filter with recon-

- figurable bandwidths using LCP multilayer circuit technology,” *IEEE Trans. Microwave Theory Tech.*, Vol. 60, No. 6, 1577–1586, 2012.
19. Chan, K. Y., S. Fouladi, R. Ramer, and R. R. Mansour, “RF MEMS switchable interdigital bandpass filter,” *IEEE Microwave and Wireless Components Letters*, Vol. 22, No. 1, 44–46, 2012.
 20. Saed, M. A., “Reconfigurable broadband microstrip antenna FED by a coplanar waveguide,” *Progress In Electromagnetics Research*, Vol. 55, 227–239, 2005.
 21. Domingue, F., S. Fouladi, A. B. Kouki, and R. R. Mansour, “Design methodology and optimization of distributed MEMS matching networks for low-microwave-frequency applications,” *IEEE Trans. Microwave Theory Tech.*, Vol. 57, No. 12, 3030–3041, 2009.
 22. Rabieirad, L. and S. Mohammadi, “Reconfigurable CMOS tuners for software-defined radio,” *IEEE Trans. Microwave Theory Tech.*, Vol. 57, No. 11, 2768–2774, 2009.
 23. Melde, K. L., H.-J. Park, H.-H. Yeh, B. Fankem, Z. Zhou, and W. R. Eisenstadt, “Software defined match control circuit integrated with a planar inverted F antenna,” *IEEE Trans. Antennas Propag.*, Vol. 58, No. 12, 3884–3890, 2010.
 24. Monti, G., R. De Paolis, and L. Tarricone, “Design of a 3-state reconfigurable CRLH transmission line based on MEMS switches,” *Progress In Electromagnetics Research*, Vol. 95, 283–297, 2009.
 25. Topalli, K., Ö. A. Çivi, Ş. Demir, S. Koc, and T. Akin, “A monolithic phased array using 3-bit distributed RF MEMS phase shifters,” *IEEE Trans. Microwave Theory Tech.*, Vol. 56, No. 2, 270–277, 2008.
 26. Qiao, D., R. Molfino, S. M. Lardizabal, B. Pillans, P. M. Asbeck, and G. Jerinic, “An intelligently controlled RF power amplifier with a reconfigurable MEMS-varactor tuner,” *IEEE Trans. Microwave Theory Tech.*, Vol. 53, No. 3, 1089–1095, 2005.
 27. Fu, C. T., C.-L. Ko, C.-N. Kuo, and Y.-Z. Juang, “A 2.4–5.4-GHz wide tuning-range CMOS reconfigurable low-noise amplifier,” *IEEE Trans. Microwave Theory Tech.*, Vol. 56, No. 12, 2754–2763, 2008.
 28. El-Nozahi, M., E. Sánchez-Sinencio, and K. Entesari, “A CMOS low-noise amplifier with reconfigurable input matching network,” *IEEE Trans. Microwave Theory Tech.*, Vol. 57, No. 5, 1054–1062, 2009.
 29. Kim, K. Y., W. Y. Kim, H. S. Son, I. Y. Oh, and C. S. Park,

- “A reconfigurable quad-band CMOS class E power amplifier for mobile and wireless applications,” *IEEE Microwave and Wireless Components Letters*, Vol. 21, No. 7, 380–382, 2011.
30. Jamlos, M. F, T. A. Rahman, M. R. Kamarudin, M. T. Ali, M. N. Md Tan, and P. Saad, “Reconfigurable aperture coupled planar antenna array at 2.3 GHz,” *PIERS Proceedings*, 573–578, Xi’an, China, Mar. 22–26, 2010.
 31. Razali, A. R. and M. E. Bialkowski, “Reconfigurable coplanar inverted-F antenna with electronically controlled ground slot,” *Progress In Electromagnetics Research B*, Vol. 34, 63–76, 2011.
 32. Persico R., N. Romano, and F. Soldovieri, “Design of a balun for a bow tie antenna in reconfigurable ground penetrating radar systems,” *Progress In Electromagnetics Research C*, Vol. 18, 123–135, 2011.
 33. Korosec, T., P. Ritos, and M. Vidmar, “Varactor-tuned microstrip-patch antenna with frequency and polarization agility,” *Electron. Lett.*, Vol. 42, No. 18, 1015–1017, 2006.
 34. Aboufoul, T., A. Alomainy, and C. Parini, “Reconfiguring UWB monopole antenna for cognitive radio applications using GaAs FET switches,” *IEEE Antennas Wireless Propag. Letters*, Vol. 11, 1392–1394, 2012.
 35. Kang, W., K. H. Ko, and K. Kim, “A compact beam reconfigurable antenna for symmetric beam switching,” *Progress In Electromagnetics Research*, Vol. 129, 1–16, 2012.
 36. Rebeiz, G. M. and J. B. Muldavin, “RF MEMS switches and switch circuits,” *IEEE Microwave Magazine*, Vol. 2, No. 4, 59–71, 2001.
 37. Bayraktar, O., O. A. Civi, and T. Akin, “Beam switching reflectarray monolithically integrated with RF MEMS switches,” *IEEE Trans. Antennas Propag.*, Vol. 60, No. 2, 854–862, 2012.
 38. Tong, K. F., K.-M. Luk, K.-F. Lee, and R. Q. Lee, “A broadband U-slot rectangular patch antenna on a microwave substrate,” *IEEE Trans. Antennas Propag.*, Vol. 48, No. 6, 854–862, 2000.
 39. Ramadan, A., K. Y. Kabalan, A. El-Hajj, S. Khoury, and M. Al-Husseini, “A reconfigurable U-Koch microstrip antenna for wireless applications,” *Progress In Electromagnetics Research*, Vol. 93, 355–367, 2009.
 40. Kim, I. and Y. Rahmat-Samii, “RF MEMS switchable slot patch antenna integrated with bias network,” *IEEE Trans. Antennas Propag.*, Vol. 59, No. 12, 4811–4815, 2011.
 41. Qin, P. Y., Y. J. Guo, A. R. Weily, and C.-H. Liang, “A pattern

- reconfigurable U-slot antenna and its applications in MIMO systems,” *IEEE Trans. Antennas Propag.*, Vol. 60, No. 2, 516–528, 2012.
42. Chang, H. P., J. Qian, B. A. Cetiner, F. De Flaviis, M. Bachman, and G. P. Li, “Design and process considerations for fabricating RF MEMS switches on printed circuit boards,” *Journal of Microelectromechanical Systems*, Vol. 14, No. 6, 1311–1322, 2005.
 43. Cetiner, B. A., L. Jofre, C. H. Chang, J. Y. Qian, M. Bachman, G. P. Li, and F. De Flaviis, “Integrated MEM antenna system for wireless communications,” *IEEE MTT-S Int. Microwave Symp. Dig.*, Vol. 14, No. 6, 1333–1337, 2002.
 44. Cetiner, B. A., J. Y. Qian, H. P. Chang, M. Bachman, G. P. Li, and F. De Flaviis, “Monolithic integration of RF MEMS switches with a diversity antenna on PCB substrate,” *IEEE Trans. Microwave Theory Tech.*, Vol. 51, 332–335, 2003.